PHYSICAL REVIEW D **82,** 052001 (2010)

Two-pion Bose-Einstein correlations in pp collisions at $\sqrt{s} = 900$ GeV

K. Aamodt *et al.**
(ALICE Collaboration)

(Received 3 July 2010; published 9 September 2010)

We report on the measurement of two-pion correlation functions from pp collisions at $\sqrt{s} = 900$ GeV performed by the ALICE experiment at the Large Hadron Collider. Our analysis shows an increase of the Hanbury Brown–Twiss radius with increasing event multiplicity, in line with other measurements done in particle- and nuclear collisions. Conversely, the strong decrease of the radius with increasing transverse momentum, as observed at the Relativistic Heavy Ion Collider and at Tevatron, is not manifest in our data.

DOI: 10.1103/PhysRevD.82.052001 PACS numbers: 25.75.Gz, 25.75.−q

I. INTRODUCTION

Proton-proton collisions at $\sqrt{s} = 900$ GeV have been recorded by ALICE (A Large Ion Collider Experiment) at the Large Hadron Collider (LHC) at CERN [1]. Hadron collisions at these energies provide an opportunity to probe quantum chromodynamics (QCD) under extreme conditions. The distinguishing feature of QCD is the mechanism of color confinement, the physics of which is not fully understood, due in part to its theoretical intractability [2]. The confinement mechanism has a physical scale on the order of the proton radius and is especially important at low momentum.

Bose-Einstein enhancement of identical-pion pairs at low relative momentum was first observed in $p\bar{p}$ collisions by Goldhaber, Goldhaber, Lee, and Pais 50 years ago [3]. Since then, two-pion correlations have been successfully applied to assess the spatial scale of the emitting source in e^+e^- [4], hadron-hadron and lepton-hadron [5], and heavy-ion [6] collisions. Especially in the latter case, this technique, known as Hanbury Brown—Twiss (HBT) interferometry [7,8] and being a special case of femtoscopy [9,10], has been developed into a precision tool to probe the dynamically generated geometry of the emitting system. In particular, a first order phase transition between the color-deconfined and -confined states was precluded by the observation of short time scales [6]. At the same time, femtoscopic measurement of bulk collective flow, manifesting itself via dynamical dependences of femtoscopic scales (“homogeneity lengths” [11,12]), provided hints that a strongly self-interacting system was created in the collision. This was further corroborated by the positive correlation between the HBT radius and the multiplicity of the event [6].

In particle physics, overviews of femtoscopic measurements in hadron- and lepton-induced collisions [4,5,13] reveal systematics surprisingly similar to those mentioned above for heavy-ion collisions. Moreover, in the first direct comparison of femtoscopy in heavy-ion collisions at the Relativistic Heavy Ion Collider (RHIC), and proton collisions in the same apparatus, a virtually identical multiplicity and momentum dependence was reported in the two systems [14].

A systematic program of femtoscopic measurements in pp and heavy-ion collisions at the LHC will shed considerable light on the nature, the similarities, and the differences of their dynamics. With the present work, we begin this program.

II. EXPERIMENT AND DATA ANALYSIS

The data discussed in this article were collected in December 2009, during the first stable-beam period of the LHC commissioning. The two beams were at the LHC injection energy of 450 GeV and each had 2–4 bunches, one of them colliding at the ALICE intersection point. The bunch intensity was typically 5×10^9 protons, giving a luminosity of the order of 10^{26} cm^{-2} s^{-1} and a rate for inelastic proton-proton collisions of a few Hz.

Approximately 3×10^5 minimum-bias pp collision events were identified by signals measured in the forward scintillators (VZERO) and the two layers of the silicon pixel detector (SPD) [15]. The VZERO counters are placed on either side of the interaction region at z = 3.3 m and z = −0.9 m. They cover the region $2.8 < \eta < 5.1$ and $-3.7 < \eta < -1.7$ and record both amplitude and time of signals produced by charged particles. The minimum-bias trigger required a hit in one of the VZERO counters or in one of the two SPD layers which cover the central pseudorapidity regions $|\eta| < 2$ (inner) and $|\eta| < 1.4$ (outer). The events were collected in coincidence with the signals from two beam pickup counters, one on each side of the interaction region, indicating the presence of passing bunches. The trigger selection efficiency for inelastic collisions was estimated to be 95–97% [16].

The VZERO counters were used also to discriminate against beam-gas and beam-halo events by requiring a strict matching between their timing signals (see Ref. [1] for details). This background was also rejected by exploiting the

*Full author list given at the end of the article.

correlation between the number of clusters of pixels and the number of tracklets pointing to a reconstructed vertex. After these selections the fraction of background events remaining in the sample of events with at least one charged-particle track was estimated to be below 0.1%. The trigger and run conditions are discussed in detail in Ref. [16].

The 250 k events used in the analysis were required to have a primary vertex (collision position) within 10 cm of the center of the 5 m long time projection chamber (TPC) [17]. This provides almost uniform acceptance for particles within the pseudorapidity range $|\eta| < 0.8$ for all events in the sample. Within this sample, we have selected events based on the measured charged-particle multiplicity M. The three multiplicity classes were $M \leq 6$, $7 \leq M \leq 11$, and $M \geq 12$; about 70% of all events were falling into the first multiplicity class. The tracks used in determining the multiplicity were the same as those used for correlation analysis (see below) except that particle identification cuts were not applied. The measured multiplicity was converted to the charged-particle pseudorapidity density $dN_{\mathrm{ch}}/d\eta$ by normalizing it to the pseudorapidity acceptance and by correcting it for the reconstruction efficiency and contamination. The correction factor was determined from a Monte Carlo simulation with the PHOJET event generator [18,19] and with the full description of the ALICE apparatus and is 0.71, 0.78, and 0.81, respectively, for the three multiplicity bins. The estimated systematic error is below 4%. The average charged-particle pseudorapidity density of the analyzed event sample is $\langle dN_{\mathrm{ch}}/d\eta \rangle = 3.6$. An alternative method based on SPD tracklets [16] gave the same result.

The ALICE TPC [17] was used to record charged-particle tracks as they leave ionization trails in the $\mathrm{Ne} - \mathrm{CO_2} - \mathrm{N_2}$ gas. The ionization electrons drift up to 2.5 m to be measured on 159 pad rows; the position resolution is better than 2 mm. Combined with a solenoidal magnetic field of B = 0.5 T this leads to a momentum resolution $\sim$1% for pions with $p_T < 1$ GeV/c. The ALICE inner tracking system (ITS) has also been used for tracking. It consists of six silicon layers, two innermost pixel detectors, two layers of drift detectors, and two outer layers of strip detectors, which provide up to six space points for each track. The tracks used in this analysis were reconstructed using the information from both the TPC (signals from at least 90 pad rows required) and the ITS. Separate studies have been done with TPC-only and ITS-only tracks, and were found to give results consistent with the combined ITS + TPC analysis. The tracks were required to project back to the primary interaction vertex within 0.2 cm (2.4 cm) in the transverse plane and 0.25 cm (3.2 cm) in the longitudinal direction, if ITS + TPC (TPC-only) information is used, thereby rejecting most secondary pions from weak decays. The pion tracks used in the correlation analysis had transverse momenta between 0.15 GeV/c and 1.0 GeV/c.

ALICE provides excellent particle identification capability. In this analysis the particle identification was achieved by correlating the magnetic rigidity of a track with its specific ionization (dE/dx) in the TPC gas. The dE/dx of the TPC was calibrated using cosmic rays and its resolution was shown to be better than 5.5%, the design value. The contamination of the pion sample is negligible within the momentum range of $0.25\ \mathrm{GeV}/c < p < 0.65\ \mathrm{GeV}/c$. Below and above this range it is on the order of 5% and is caused by electrons and kaons, respectively.

III. TWO-PION CORRELATION FUNCTIONS

The two-particle correlation function is defined as the ratio $C(\mathbf{q}) = A(\mathbf{q})/B(\mathbf{q})$, where $A(\mathbf{q})$ is the measured distribution of pair momentum difference $\mathbf{q} = \mathbf{p}_2 - \mathbf{p}_1$, and $B(\mathbf{q})$ is a similar distribution formed by using pairs of particles from different events (event mixing) [20]. The limited statistics available (520 k identical-pion pairs with $q_{\mathrm{inv}} < 0.5$ GeV/c) allowed us to perform a detailed analysis only for the one-dimensional two-pion correlation function $C(q_{\mathrm{inv}})$. The q_{inv} is, for identical mass particles, equal to the modulus of the momentum difference $|\mathbf{q}|$ in the pair rest frame.

The correlation functions were studied in bins of event multiplicity and of transverse momentum, defined as half of the vector sum of the two transverse momenta, $k_T = |\mathbf{p}_{T,1} + \mathbf{p}_{T,2}|/2$. During event mixing, all pion tracks from one event were paired with all pion tracks from another event. Every event was mixed with five other events with similar multiplicities; ten multiplicity bins were introduced for this purpose. The multiplicity binning improved the flatness of the correlation function at $q_{\mathrm{inv}} > 1.5$ GeV/c. Binning events according to their vertex position, on the other hand, had no effect on the correlation function and therefore was not used. Alternatively to event mixing, the denominator can be obtained by rotating one of the two tracks by 180° in azimuth. The correlation functions obtained using this technique are generally flatter at high q_{inv} than those from event mixing. The difference between the results obtained utilizing the two techniques was used in estimating the systematic errors.

For the correlation structures measured here, with characteristic widths $\sim$0.2 GeV/c, track splitting and track merging in the event reconstruction are small effects overall. Their impact on the results was carefully studied with the Monte Carlo simulation and turned out to be negligible.

Another apparatus effect considered is the momentum resolution. Momentum smearing for single particles has a similar effect on the correlation structures in two-particle correlations, i.e., it smears the correlation peak, making it appear lower and wider. We have studied this effect with the Monte-Carlo simulation of the ALICE detector and have found that for the width of the correlation peak expected here the effect is on the order of 1%.

Figure 1 presents two-pion correlation functions measured by ALICE in pp collisions at $\sqrt{s} = 900$ GeV, as a function of event multiplicity and transverse momentum

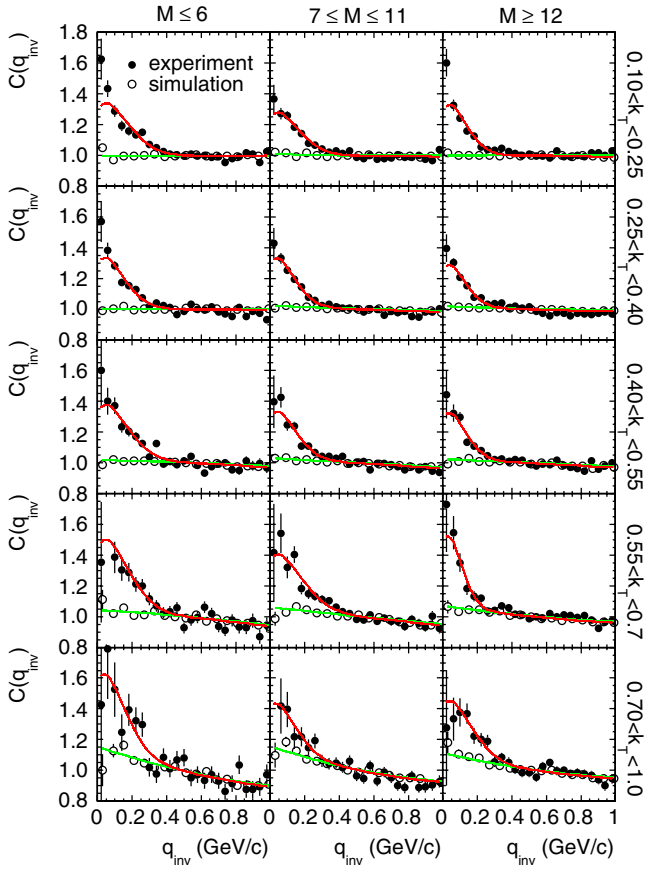

FIG. 1 (color online). Correlation functions for identical pions from pp collisions at $\sqrt{s} = 900$ GeV (full dots) and those obtained from a simulation using PHOJET (open circles). Positive and negative pion pairs were combined. The three columns represent collisions with different charged-particle multiplicities M; the transverse momentum of pion pairs k_T (GeV/c) increases from top to bottom. The lines going through the points represent the Gaussian fits discussed in the text.

k_T. The denominator of the correlation function was obtained via event mixing and normalized such that the numbers of true and mixed pairs with $0.4\ \mathrm{GeV}/c < q_{\mathrm{inv}} < 0.6\ \mathrm{GeV}/c$ were equal. The q_{inv} range used for normalization was chosen to be outside of the Bose-Einstein peak but as close as possible to it. The normalized distributions of positive and negative pion pairs were added together before building the ratio of true and mixed pairs. The Bose-Einstein enhancement is manifest at low q_{inv}. A slight decrease of the correlation peak width is seen as multiplicity grows. The k_T dependence is less obvious because the correlation baseline—the underlying two-particle correlation without any Bose-Einstein enhancement—is systematically changing its shape between the low and high transverse momenta.

The correlation functions were fitted by a function accounting for the Bose-Einstein enhancement and for the mutual Coulomb interaction between the two particles:

$$C(q_{\mathrm{inv}}) = ((1-\lambda) + \lambda K(q_{\mathrm{inv}}) \times [1 + \exp(-R_{\mathrm{inv}}^2 q_{\mathrm{inv}}^2)])D(q_{\mathrm{inv}}), \quad (1)$$

with λ describing the correlation strength and R_{inv} being the Gaussian HBT radius [21]. The factor K is the Coulomb function integrated over a spherical source of the size 1 fm. It is attenuated by the same factor λ as the Bose-Einstein peak. The factor $D(q_{\mathrm{inv}})$ accounts for long-range correlations, like those arising from jets and/or from energy and momentum conservation, and plays an important role in the analysis as will be discussed later.

Neglecting the Coulomb interaction $K(q_{\mathrm{inv}}) \equiv 1$ the fit function reduces to

$$C(q_{\mathrm{inv}}) = [1 + \lambda \exp(-R_{\mathrm{inv}}^2 q_{\mathrm{inv}}^2)]D(q_{\mathrm{inv}}). \quad (2)$$

The difference between the R_{inv} values obtained with and without the Coulomb correction is less than 0.05 fm.

While the Gaussian fit captures the bulk scales of the correlation, at low q_{inv} the data points lie above the fit line. This feature was observed previously in pion correlations from particle collisions. An exponential fit

$$C(q_{\mathrm{inv}}) = [1 + \lambda \exp(-R_{\mathrm{inv}} q_{\mathrm{inv}})]D(q_{\mathrm{inv}}) \quad (3)$$

matches the data better. However, contrary to the Gaussian R_{inv}, the R_{inv} parameter from Eq. (3) does not have a straightforward interpretation as the "radius of the source." We have used both functional forms and leave a detailed investigation of the correlation peak shape to future studies. In order to make the connection to established systematics at lower energy particle and heavy-ion collisions, a careful treatment of the long-range correlations, visible as a slope in the baseline of the correlation developing with increasing transverse momentum and represented by the factor $D(q_{\mathrm{inv}})$ in Eqs. (1)–(3), is crucial.

In order to better understand the shape of the correlation baseline we have calculated correlation functions for pp collisions events generated by the model PHOJET and propagated through the ALICE detectors, performing an identical analysis for the simulated events as for the measured ones. The results are shown as open circles in Fig. 1. The model does not contain the Bose-Einstein effect, hence the lack of the peak at low q_{inv} is expected. At low k_T and low multiplicity, the model predicts a flat correlation function. However, as k_T increases, long-range correlations start becoming visible as a distortion of the correlation function baseline similar to that seen in the experimental data.

The accuracy of our simulation in describing the correlation baseline was verified with unlike-sign pion pairs. The multiplicity and k_T dependence of the $\pi^+\pi^-$ functions is shown in Fig. 2. Correlation structures for nonidentical pions include a mutual Coulomb interaction peak, here limited to the first bin at lowest q_{inv}, and peaks coming from meson decays which should be correctly modeled in the event generator. Therefore, one can directly

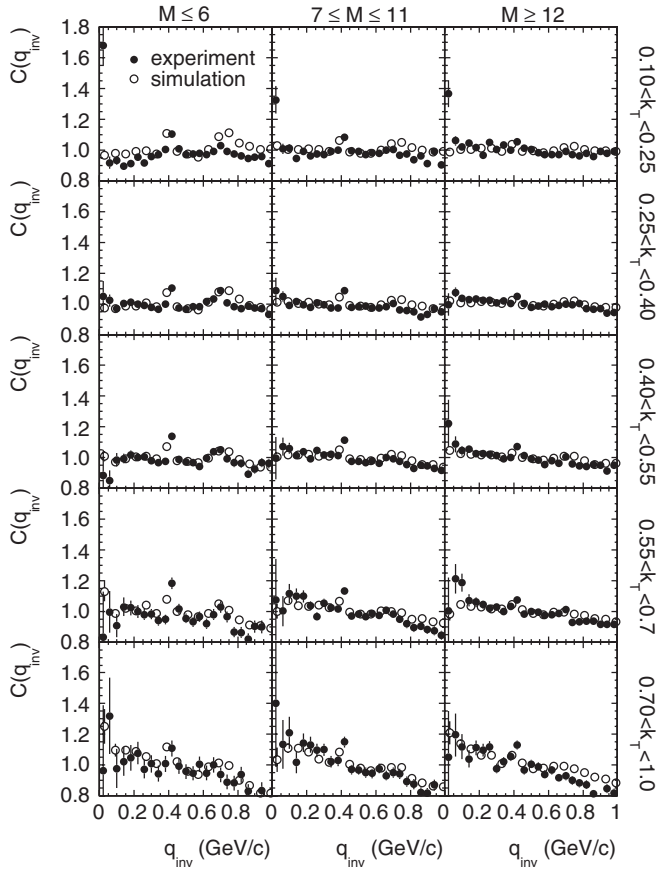

FIG. 2. One-dimensional correlation functions for $\pi^+\pi^-$ pairs from pp collisions at $\sqrt{s} = 900$ GeV. The columns and rows are defined as in Fig. 1.

compare simulations with data. In Fig. 2, the simulated correlation functions agree reasonably well with the experimental data. This suggests that the same model (PHOJET) can be used as a reasonable estimate also for identical particles to describe the correlation baseline under the Bose-Einstein peak. The presence of resonance peaks (like the K^0_S one at $q_{\rm inv} = 412$ MeV$/c$) and the fact that the simulated correlations for identical and nonidentical-pion pairs have different slopes, on the other hand, indicate that unlike-sign pion pairs cannot be directly used for the denominator of the identical-pion correlations.

The procedure employed to extract the HBT radii with Eq. (1) using the PHOJET baseline is as follows. First, the simulation points shown in Fig. 1 are fitted with the 2nd-order polynomial

$$D(q_{\rm inv}) = a + bq_{\rm inv} + cq^2_{\rm inv}. \quad (4)$$

Subsequently, the experimental correlation function is fitted by Eq. (1), taking the $D(q_{\rm inv})$ from the PHOJET fit and adjusting λ and $R_{\rm inv}$. The two fits are represented in Fig. 1 by the lines going through the simulation and experiment data points, respectively.

In order to estimate the systematic error from the baseline determination we repeated the fitting procedure using a simulation performed with the PYTHIA [22] generator [version 6.4.21, Perugia-0 (320) tune [23]] instead of PHOJET. The HBT radii obtained in the two ways differ by up to 10%. In the following we use the average between them and we estimate the systematic error related to the baseline shape assumption to be half of the difference.

It is interesting to see what happens with the radii if the slope of the baseline is neglected. Assuming a flat baseline $D(q_{\rm inv}) \equiv a$ and treating a as the third fit parameter in Eq. (1) leads to $R_{\rm inv}$ values that are similar to those obtained with the PHOJET or the PYTHIA baseline at low k_T values but smaller by up to 30% at high transverse momenta. This is because the broad enhancement caused by long-range correlations will be attributed to Bose-Einstein correlations, giving rise to smaller radii (wider correlation function). The resulting apparent k_T dependence will be discussed in Sec. V.

The $R_{\rm inv}$ obtained from the fit (the two highest multiplicity bins combined) is shown in Fig. 3. In order to reduce the statistical errors and to compare to other experiments, in the following sections of this article we analyze separately the multiplicity and the transverse momentum dependences.

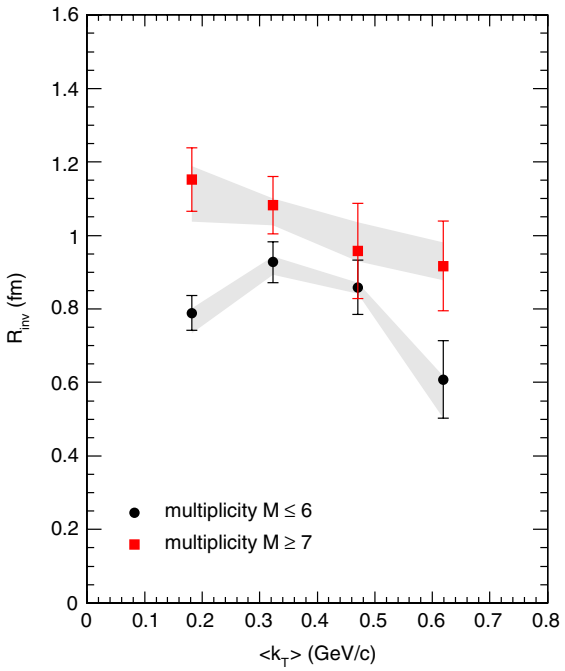

FIG. 3 (color online). Extracted HBT radius as a function of k_T for low (black circles) and high (red squares) multiplicity events. The error bars are statistical. The shaded bands represent the systematic errors related to the baseline shape assumption and to the fit range, added in quadrature.

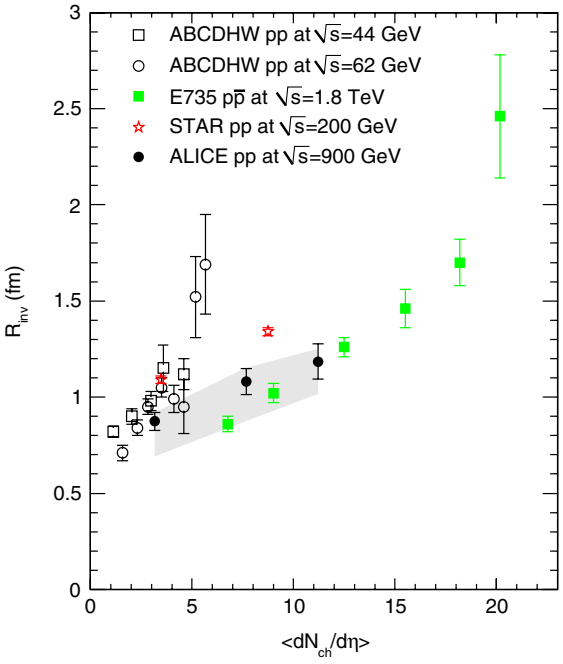

FIG. 4 (color online). One-dimensional Gaussian HBT radius in pp collisions at $\sqrt{s} = 900$ GeV determined using pion pairs with $k_T = 0.1$–0.55 GeV/c, $\langle k_T \rangle = 0.32$ GeV/c, and shown as a function of the charged-particle multiplicity at midrapidity (full dots). The shaded band represents the systematic errors (see text). For comparison, open symbols, red stars, and green filled boxes represent the data taken at the ISR [24], RHIC [14], and Tevatron [25], respectively.

IV. MULTIPLICITY DEPENDENCE OF THE HBT RADIUS

The multiplicity dependence of the obtained HBT radius is shown in Fig. 4 and Table I. The analysis here was restricted to the first three transverse momentum bins $k_T = 0.1$–0.55 GeV/c. The mean transverse momentum for pairs with $q_{\rm inv} < 0.2$ GeV/c is $\langle k_T \rangle = 0.32$ GeV/c. The HBT radii were obtained by using PHOJET and PYTHIA to estimate the shape of the baseline, as explained in the previous section. The systematic errors related to the baseline assumption reflect the difference between the two. The systematic error related to the choice of the normalization and/or fit range was estimated to be 5%. An additional downward systematic error of 13–20% accounts for the difference between the event mixing and the rotation denominator techniques. The shaded area represents the three systematic errors added in quadrature.

TABLE I. One-dimensional HBT radius in pp collisions at $\sqrt{s} = 900$ GeV determined using pion pairs with $k_T = 0.1$–0.55 GeV/c, $\langle k_T \rangle = 0.32$ GeV/c, as a function of the charged-particle pseudorapidity density at midrapidity. The radii were obtained using the Gaussian fit function defined by Eq. (1).

$\langle dN_{\rm ch}/d\eta \rangle$	λ	$R_{\rm inv}$ (fm)
3.2	0.386 ± 0.022	$0.874 \pm 0.047({\rm stat})^{+0.047}_{-0.181}({\rm syst})$
7.7	0.331 ± 0.023	$1.082 \pm 0.068({\rm stat})^{+0.069}_{-0.206}({\rm syst})$
11.2	0.310 ± 0.026	$1.184 \pm 0.092({\rm stat})^{+0.067}_{-0.168}({\rm syst})$

The charged-particle pseudorapidity density $\langle dN_{\rm ch}/d\eta \rangle$ of the lowest multiplicity bin was calculated excluding events with multiplicities $M < 2$ because these events do not contribute to the numerator of the correlation function. Including all events and including only events with at least one like-sign pair would shift the point by 0.8 to the left and to the right, respectively.

An increase of the HBT radius with multiplicity is observed, consistent with the hadron-hadron collision systematics above $\sqrt{s} \sim 50$ GeV [13]. While the average transverse momentum is similar in all four data sets, other aspects of the analysis, e.g., the average orientation of the momentum difference vector, can differ so the trends, not the absolute values, should be compared. In heavy-ion collisions, this multiplicity dependence has been associated with the particle composition and overall volume of the final-state system [6,26,27] or with final-state hadronic rescattering [28]. The relation observed in heavy-ion collision data [6], $R \sim a + b(dN_{\rm ch}/d\eta)^{1/3}$, where a and b are constants, appears to be consistent with our data within our systematic errors. For high-energy pp collisions, it has been suggested that a similar behavior could originate from final-state hadronic rescattering for short hadronization times [29]. In an alternative scenario, the increase of the HBT radius with multiplicity results from the fact that the high multiplicity pp events mostly come from hard parton scattering, and the hadronization length, i.e., the distance travelled by a parton before hadronization, is roughly proportional to the parton energy [30].

The fitted correlation strength λ is lower than unity, the value expected for the ideal Bose-Einstein case. One reason for this is the non-Gaussian shape of the peak, caused at least partially by pions from decays of short-(Δ, ρ) and long-lived resonances (ω, η, η'). On the detector side, λ can be reduced by the particle misidentification; this effect is, however, small in our data sample. In ALICE, λ decreases from 0.37 ± 0.03 to 0.32 ± 0.03 between the lowest and the highest multiplicity, in close agreement with the E735 measurements at Tevatron [25]. A similar trend was observed by UA1 in $p\bar{p}$ collisions at $\sqrt{s} = 630$ GeV/c [31]; the fact that their λ values were lower may have to do with the lack of the particle identification and the resulting dilution of the correlation peak. In a final-state hadronic rescattering model [29], a correlation strength dropping with multiplicity in high-energy pp collisions was attributed to the increased contribution from long-lived resonances in higher multiplicity events.

An increase of the HBT radius with increasing particle multiplicity was recently reported by the CMS Collaboration for the same collision system and energy [32]. The authors fit the correlation peak by an exponential

TABLE II. One-dimensional HBT radius in pp collisions at $\sqrt{s} = 900$ GeV determined using pion pairs with $k_T = 0.1$–0.55 GeV/c, $\langle k_T \rangle = 0.32$ GeV/c, as a function of the charged-particle pseudorapidity density at midrapidity. The radii were obtained using the exponential fit function defined by Eq. (3).

$\langle dN_{\rm ch}/d\eta \rangle$	λ	$R_{\rm inv}/\sqrt{\pi}$ (fm)
3.2	0.704 ± 0.048	$0.809 \pm 0.061(\text{stat})^{+0.049}_{-0.208}(\text{syst})$
7.7	0.577 ± 0.054	$0.967 \pm 0.095(\text{stat})^{+0.071}_{-0.206}(\text{syst})$
11.2	0.548 ± 0.051	$1.069 \pm 0.104(\text{stat})^{+0.063}_{-0.203}(\text{syst})$

[Eq. (3)]. An analogous approach in our case (Table II) yields radii that are rather similar to the Gaussian ones (Table I) once scaled down by $\sqrt{\pi}$ [32]. In order to compare between the two experiments we perform a fit to an inclusive correlation (all multiplicities and k_T's). The exponential fit to the correlation functions obtained using event mixing and using rotation yields $R_{\rm inv} = 1.61 \pm 0.07(\text{stat}) \pm 0.05(\text{syst})$ fm and $R_{\rm inv} = 1.31 \pm 0.05(\text{stat}) \pm 0.22(\text{syst})$ fm, respectively. This is in close agreement with the corresponding values quoted by CMS, 1.72 ± 0.06 fm and 1.29 ± 0.04 fm.

V. TRANSVERSE MOMENTUM DEPENDENCE OF THE HBT RADIUS

One of the key features of the bulk system created in nuclear collisions is its large collective flow. The fingerprint of this flow is a specific space-momentum correlation signature, revealed in the transverse momentum dependence of the Gaussian HBT radius [6]. While quantitative comparison between particle and heavy-ion studies is complicated by experiments using different acceptances and techniques, a recent comparison of the HBT radii from pp and Au + Au collisions at RHIC indicates an almost identical p_T dependence between these collision systems [14]. Again, this raises the interesting question of whether hadron collisions at the highest energies already develop a bulk, collective behavior.

The k_T dependence of our measured HBT radius is shown in Fig. 5. The choice of the fitting method, which only weakly affects the multiplicity dependence of the HBT radius discussed in the previous section, is of crucial importance for the transverse momentum dependence. Taking the baseline shape from the Monte Carlo leads to an HBT radius that is nearly independent of k_T (filled black circles and red boxes for PHOJET and PYTHIA, respectively). Assuming a flat baseline, on the other hand, results in a radius falling with k_T (green stars). As discussed in the previous section, the experimental unlike-sign pion correlation functions are close to the predictions of PHOJET and PYTHIA and we consider using the average between the two cases as baseline to be a reliable estimate for the HBT radii.

The radii obtained in this fashion are summarized in Tables III and IV and shown in Fig. 6 where we compare

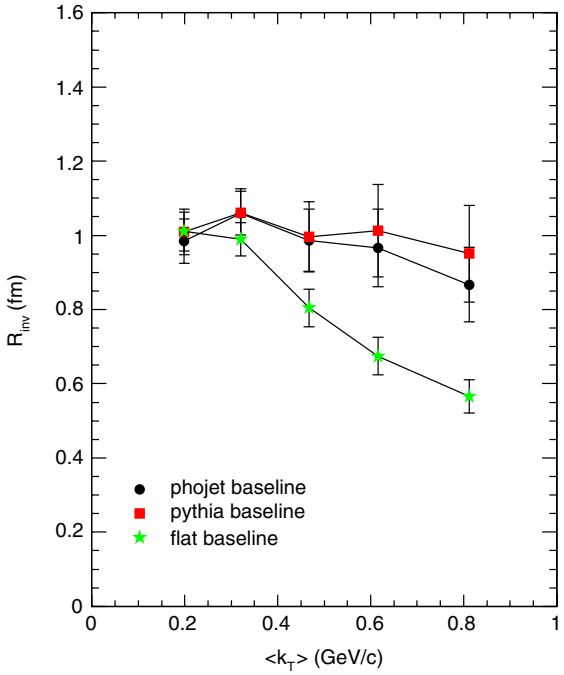

FIG. 5 (color online). One-dimensional Gaussian HBT radius in pp collisions at $\sqrt{s} = 900$ GeV as a function of transverse momentum k_T. Three fitting methods, differing by the choice of the baseline parametrization, are compared.

them to RHIC and Tevatron data [13]. As with the multiplicity dependence, the systematic error band represents a quadratic sum of the error related to the baseline assumption (0–10%), the fit range (10%), and the denominator construction method (mixing/rotating, 7–17%). The lowest-k_T point is significantly below the RHIC and

TABLE III. One-dimensional HBT radius in pp collisions at $\sqrt{s} = 900$ GeV as a function of the pair k_T. The radii were obtained using the Gaussian fit function defined by Eq. (1).

$\langle k_T \rangle$ (GeV/c)	λ	$R_{\rm inv}$ (fm)
0.20	0.35 ± 0.03	$1.00 \pm 0.06(\text{stat})^{+0.10}_{-0.20}(\text{syst})$
0.32	0.33 ± 0.03	$1.06 \pm 0.06(\text{stat})^{+0.11}_{-0.19}(\text{syst})$
0.47	0.30 ± 0.04	$0.99 \pm 0.09(\text{stat})^{+0.10}_{-0.14}(\text{syst})$
0.62	0.35 ± 0.06	$0.99 \pm 0.11(\text{stat})^{+0.10}_{-0.13}(\text{syst})$
0.81	0.31 ± 0.06	$0.91 \pm 0.12(\text{stat})^{+0.10}_{-0.12}(\text{syst})$

TABLE IV. One-dimensional HBT radius in pp collisions at $\sqrt{s} = 900$ GeV as a function of the pair k_T. The radii were obtained using the exponential fit function defined by Eq. (3).

$\langle k_T \rangle$ (GeV/c)	λ	$R_{\rm inv}/\sqrt{\pi}$ (fm)
0.20	0.63 ± 0.05	$0.94 \pm 0.07(\text{stat})^{+0.09}_{-0.20}(\text{syst})$
0.32	0.58 ± 0.04	$0.93 \pm 0.07(\text{stat})^{+0.09}_{-0.20}(\text{syst})$
0.47	0.55 ± 0.07	$0.92 \pm 0.10(\text{stat})^{+0.09}_{-0.14}(\text{syst})$
0.62	0.70 ± 0.11	$0.98 \pm 0.14(\text{stat})^{+0.10}_{-0.14}(\text{syst})$
0.81	0.60 ± 0.12	$0.90 \pm 0.16(\text{stat})^{+0.12}_{-0.15}(\text{syst})$

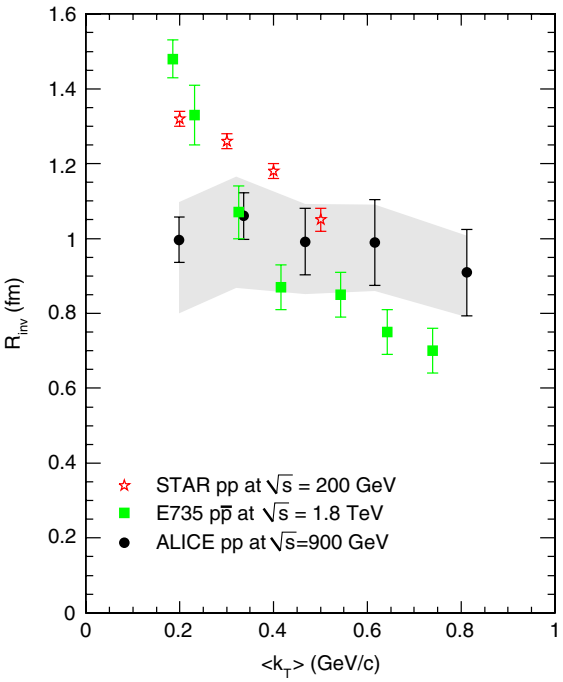

FIG. 6 (color online). One-dimensional Gaussian HBT radius in pp collisions at $\sqrt{s} = 900$ GeV as a function of transverse momentum k_T (full dots). The mean charged-particle multiplicity density was $\langle dN_{\rm ch}/d\eta \rangle = 3.6$. The systematic errors are indicated by the shaded area. Stars and filled boxes represent the radii measured at RHIC [14] and Tevatron [25], respectively.

Tevatron results. It should be noted that the ALICE analysis was performed on a minimum-bias event sample and the averaged charged-particle pseudorapidity density is $\langle dN_{\rm ch}/d\eta \rangle = 3.6$ while the Tevatron events are biased to high multiplicity, $\langle dN_{\rm ch}/d\eta \rangle = 14.4$, similar to our highest multiplicity bin. As visible in Fig. 3, the lowest-k_T point at the high multiplicity is at $R_{\rm inv} \approx 1.2$ fm, approaching the Tevatron points. The STAR results, on the other hand, were obtained from events with $\langle dN_{\rm ch}/d\eta \rangle = 4.3$, i.e., similar to the ALICE case and thus a similar reasoning cannot explain the difference.

Two tests were performed to make sure that the low HBT radius value at low transverse momenta is not caused by apparatus effects. First, the analysis was repeated using only the ITS and thus reducing the low-momentum cutoff by about 50 MeV/c. This analysis yielded the same HBT radius which demonstrates that the energy loss is not an issue. Second, as seen in Fig. 3 the low-k_T point is mostly driven down by the contribution of the low-multiplicity events. Since the vertex resolution in these events is worse this might in principle deteriorate the momentum resolution and smear out the correlation function peak. In order to test this, the analysis was performed without using the event vertex constraint for momentum determination. The results, again, were unchanged. This, and the distinct K^0_S peak in the unlike-sign pion correlation functions in the low-multiplicity low-k_T bin of Fig. 2, indicate that the momentum resolution is not spoiled in low-multiplicity events.

Even more important than the position of the first point, albeit related to it, is the question of the slope of the points in Fig. 6. Our measured HBT radius is practically independent of k_T within the studied transverse momentum range. The slope crucially depends on the baseline shape assumption, as was shown in Fig. 5. The results from the experiments to which we are comparing in Fig. 6 were extracted using a flat background (although the STAR experiment also studied the effects of using other types of backgrounds for their data to account for the nonfemtoscopic effects [14]). Assuming that PHOJET and PYTHIA are correct such a procedure may lead to a misinterpretation of the low-q enhancement of the correlation function, that is coming from long-range correlations (most probably minijet like), as a Bose-Einstein enhancement. As the impact of this may depend on the details of each experiment (certainly on the collision energy) we do not attempt to resolve this question quantitatively. However, we stress again the usefulness of nonidentical-pion correlation in constraining the correlation baseline.

VI. SUMMARY

In summary, ALICE has measured two-pion correlation functions in pp collisions at $\sqrt{s} = 900$ GeV at the LHC. Consistent with previous measurements of high-energy hadron-hadron and nuclear collisions, the extracted HBT radius $R_{\rm inv}$ increases with event multiplicity. Less consistent is the relation between $R_{\rm inv}$ and the pion transverse momentum where the ALICE measured HBT radius in minimum-bias events is practically constant within our errors and within the transverse momentum range studied.

ACKNOWLEDGMENTS

The ALICE collaboration would like to thank all its engineers and technicians for their invaluable contributions to the construction of the experiment and the CERN accelerator teams for the outstanding performance of the LHC complex. The ALICE collaboration acknowledges the following funding agencies for their support in building and running the ALICE detector: Calouste Gulbenkian Foundation from Lisbon and Swiss Fonds Kidagan, Armenia; Conselho Nacional de Desenvolvimento Científico e Tecnológico (CNPq), Financiadora de Estudos e Projetos (FINEP), Fundação de Amparo à Pesquisa do Estado de São Paulo (FAPESP); National Natural Science Foundation of China (NSFC), the Chinese Ministry of Education (CMOE) and the Ministry of Science and Technology of China (MSTC); Ministry of Education and Youth of the Czech Republic; Danish Natural Science Research Council, the Carlsberg Foundation and the Danish National Research

Foundation; The European Research Council under the European Community's Seventh Framework Programme; Helsinki Institute of Physics and the Academy of Finland; French CNRS-IN2P3, the "Region Pays de Loire," "Region Alsace," "Region Auvergne," and CEA, France; German BMBF and the Helmholtz Association; Hungarian OTKA and National Office for Research and Technology (NKTH); Department of Atomic Energy and Department of Science and Technology of the Government of India; Istituto Nazionale di Fisica Nucleare (INFN) of Italy; MEXT Grant-in-Aid for Specially Promoted Research, Japan; Joint Institute for Nuclear Research, Dubna; Korea Foundation for International Cooperation of Science and Technology (KICOS); CONACYT, DGAPA, México, ALFA-EC and the HELEN Program (High-Energy physics Latin American European Network); Stichting voor Fundamenteel Onderzoek der Materie (FOM) and the Nederlandse Organisatie voor Wetenschappelijk Onderzoek (NWO), Netherlands; Research Council of Norway (NFR); Polish Ministry of Science and Higher Education; National Authority for Scientific Research-NASR (Autoritatea Naţională pentru Cercetare Ştiinţifică-ANCS); Federal Agency of Science of the Ministry of Education and Science of Russian Federation, International Science and Technology Center, Russian Academy of Sciences, Russian Federal Agency of Atomic Energy, Russian Federal Agency for Science and Innovations and CERN-INTAS; Ministry of Education of Slovakia; CIEMAT, EELA, Ministerio de Educacíon y Ciencia of Spain, Xunta de Galicia (Consellería de Educacíon), CEADEN, Cubaenergía, Cuba, and IAEA (International Atomic Energy Agency); Swedish Reseach Council (VR) and Knut & Alice Wallenberg Foundation (KAW); Ukraine Ministry of Education and Science; United Kingdom Science and Technology Facilities Council (STFC); The United States Department of Energy, the United States National Science Foundation, the State of Texas, and the State of Ohio.

[1] ALICE Collaboration, Eur. Phys. J. C **65**, 111 (2010).
[2] A. Peshier, B. Kämpfer, and G. Soff, Phys. Rev. D **66**, 094003 (2002).
[3] G. Goldhaber, S. Goldhaber, W.-Y. Lee, and A. Pais, Phys. Rev. **120**, 300 (1960).
[4] W. Kittel, Acta Phys. Pol. B **32**, 3927 (2001).
[5] G. Alexander, Rep. Prog. Phys. **66**, 481 (2003).
[6] M. A. Lisa, S. Pratt, R. Soltz, and U. Wiedemann, Annu. Rev. Nucl. Part. Sci. **55**, 357 (2005).
[7] R. Hanbury Brown and R. Q. Twiss, Nature (London) **178**, 1046 (1956).
[8] R. Hanbury Brown and R. Q. Twiss, Philos. Mag. **45**, 663 (1954).
[9] R. Lednicky and V. L. Lyuboshits, in *Proceedings of the International Workshop on Particle Correlations and Interferometry in Nuclear Collisions, Nantes, France*, edited by D. Ardouin (World Scientific, Singapore, 1990), p. 42–54.
[10] R. Lednicky, arXiv:nucl-th/0212089.
[11] S. V. Akkelin and Y. M. Sinyukov, Phys. Lett. B **356**, 525 (1995).
[12] Y. M. Sinyukov, Nucl. Phys. **A566**, 589 (1994).
[13] Z. Chajęcki, Acta Phys. Pol. B **40**, 1119 (2009).
[14] M. M. Aggarwal *et al.* (STAR Collaboration), arXiv:1004.0925.
[15] K. Aamodt *et al.* (ALICE Collaboration), JINST **3**, S08002 (2008).
[16] K. Aamodt *et al.* (ALICE Collaboration), Eur. Phys. J. C **68**, 89 (2010).
[17] J. Alme *et al.*, arXiv:1001.1950.
[18] R. Engel, Z. Phys. C **66**, 203 (1995).
[19] R. Engel and J. Ranft, Phys. Rev. D **54**, 4244 (1996).
[20] G. I. Kopylov, Phys. Lett. **50B**, 472 (1974).
[21] Y. Sinyukov, R. Lednicky, S. V. Akkelin, J. Pluta, and B. Erazmus, Phys. Lett. B **432**, 248 (1998).
[22] T. Sjöstrand, S. Mrenna, and P. Skands, J. High Energy Phys. 05 (2006) 026.
[23] P. Z. Skands, arXiv:0905.3418.
[24] A. Breakstone *et al.* (Ames-Bologna-CERN-Dortmund-Heidelberg-Warsaw Collaboration), Z. Phys. C **33**, 333 (1987).
[25] T. Alexopoulos *et al.*, Phys. Rev. D **48**, 1931 (1993).
[26] D. Antończyk and D. Miśkowiec, Braz. J. Phys. **37**, 979 (2007).
[27] D. Adamová *et al.* (CERES Collaboration), Phys. Rev. Lett. **90**, 022301 (2003).
[28] T. J. Humanic, Phys. Rev. C **79**, 044902 (2009).
[29] T. J. Humanic, Phys. Rev. C **76**, 025205 (2007).
[30] G. Paić and P. K. Skowroński, J. Phys. G **31**, 1045 (2005).
[31] C. Albajar *et al.* (UA1 Collaboration), Phys. Lett. B **226**, 410 (1989).
[32] V. Khachatryan *et al.* (CMS Collaboration), Phys. Rev. Lett. **105**, 032001 (2010).

K. Aamodt,[1] N. Abel,[2] U. Abeysekara,[3] A. Abrahantes Quintana,[4] A. Abramyan,[5] D. Adamová,[6] M. M. Aggarwal,[7] G. Aglieri Rinella,[8] A. G. Agocs,[9] S. Aguilar Salazar,[10] Z. Ahammed,[11] A. Ahmad,[12] N. Ahmad,[12] S. U. Ahn,[13,b] R. Akimoto,[14] A. Akindinov,[15] D. Aleksandrov,[16] B. Alessandro,[17] R. Alfaro Molina,[10] A. Alici,[18] E. Almaráz Aviña,[10] J. Alme,[19] T. Alt,[2,c] V. Altini,[20] S. Altinpinar,[21] C. Andrei,[22] A. Andronic,[21] G. Anelli,[8]

V. Angelov,[2,c] C. Anson,[23] T. Antičić,[24] F. Antinori,[8,d] S. Antinori,[18] K. Antipin,[25] D. Antończyk,[25] P. Antonioli,[26] A. Anzo,[10] L. Aphecetche,[27] H. Appelshäuser,[25] S. Arcelli,[18] R. Arceo,[10] A. Arend,[25] N. Armesto,[28] R. Arnaldi,[17] T. Aronsson,[29] I. C. Arsene,[1,e] A. Asryan,[30] A. Augustinus,[8] R. Averbeck,[21] T. C. Awes,[31] J. Äystö,[32] M. D. Azmi,[12] S. Bablok,[19] M. Bach,[33] A. Badalà,[34] Y. W. Baek,[13,b] S. Bagnasco,[17] R. Bailhache,[21,f] R. Bala,[35] A. Baldisseri,[36] A. Baldit,[37] J. Bán,[38] R. Barbera,[39] G. G. Barnaföldi,[9] L. S. Barnby,[40] V. Barret,[37] J. Bartke,[41] F. Barile,[20] M. Basile,[18] V. Basmanov,[42] N. Bastid,[37] B. Bathen,[43] G. Batigne,[27] B. Batyunya,[44] C. Baumann,[43,f] I. G. Bearden,[45] B. Becker,[46,g] I. Belikov,[47] R. Bellwied,[48] E. Belmont-Moreno,[10] A. Belogianni,[49] L. Benhabib,[27] S. Beole,[35] I. Berceanu,[22] A. Bercuci,[21,h] E. Berdermann,[21] Y. Berdnikov,[50] L. Betev,[8] A. Bhasin,[51] A. K. Bhati,[7] L. Bianchi,[35] N. Bianchi,[52] C. Bianchin,[53] J. Bielčík,[54] J. Bielčíková,[6] A. Bilandzic,[55] L. Bimbot,[56] E. Biolcati,[35] A. Blanc,[37] F. Blanco,[39,i] F. Blanco,[57] D. Blau,[16] C. Blume,[25] M. Boccioli,[8] N. Bock,[23] A. Bogdanov,[58] H. Bøggild,[45] M. Bogolyubsky,[59] J. Bohm,[60] L. Boldizsár,[9] M. Bombara,[61] C. Bombonati,[53,j] M. Bondila,[32] H. Borel,[36] A. Borisov,[62] C. Bortolin,[53,k] S. Bose,[63] L. Bosisio,[64] F. Bossú,[35] M. Botje,[55] S. Böttger,[2] G. Bourdaud,[27] B. Boyer,[56] M. Braun,[30] P. Braun-Munzinger,[21,65,c] L. Bravina,[1] M. Bregant,[64,l] T. Breitner,[2] G. Bruckner,[8] R. Brun,[8] E. Bruna,[29] G. E. Bruno,[20] D. Budnikov,[42] H. Buesching,[25] P. Buncic,[8] O. Busch,[66] Z. Buthelezi,[67] D. Caffarri,[53] X. Cai,[68] H. Caines,[29] E. Calvo,[69] E. Camacho,[70] P. Camerini,[64] M. Campbell,[8] V. Canoa Roman,[8] G. P. Capitani,[52] G. Cara Romeo,[26] F. Carena,[8] W. Carena,[8] F. Carminati,[8] A. Casanova Díaz,[52] M. Caselle,[8] J. Castillo Castellanos,[36] J. F. Castillo Hernandez,[21] V. Catanescu,[22] E. Cattaruzza,[64] C. Cavicchioli,[8] P. Cerello,[17] V. Chambert,[56] B. Chang,[60] S. Chapeland,[8] A. Charpy,[56] J. L. Charvet,[36] S. Chattopadhyay,[63] S. Chattopadhyay,[11] M. Cherney,[3] C. Cheshkov,[8] B. Cheynis,[71] E. Chiavassa,[35] V. Chibante Barroso,[8] D. D. Chinellato,[72] P. Chochula,[8] K. Choi,[73] M. Chojnacki,[74] P. Christakoglou,[74] C. H. Christensen,[45] P. Christiansen,[75] T. Chujo,[76] F. Chuman,[77] C. Cicalo,[46] L. Cifarelli,[18] F. Cindolo,[26] J. Cleymans,[67] O. Cobanoglu,[35] J.-P. Coffin,[47] S. Coli,[17] A. Colla,[8] G. Conesa Balbastre,[52] Z. Conesa del Valle,[27,m] E. S. Conner,[78] P. Constantin,[66] G. Contin,[64,j] J. G. Contreras,[70] Y. Corrales Morales,[35] T. M. Cormier,[48] P. Cortese,[79] I. Cortés Maldonado,[80] M. R. Cosentino,[72] F. Costa,[8] M. E. Cotallo,[57] E. Crescio,[70] P. Crochet,[37] E. Cuautle,[81] L. Cunqueiro,[52] J. Cussonneau,[27] A. Dainese,[82] H. H. Dalsgaard,[45] A. Danu,[83] I. Das,[63] A. Dash,[84] S. Dash,[84] G. O. V. de Barros,[85] A. De Caro,[86] G. de Cataldo,[87] J. de Cuveland,[2,c] A. De Falco,[88] M. De Gaspari,[66] J. de Groot,[8] D. De Gruttola,[86] N. De Marco,[17] S. De Pasquale,[86] R. De Remigis,[17] R. de Rooij,[74] G. de Vaux,[67] H. Delagrange,[27] Y. Delgado,[69] G. Dellacasa,[79] A. Deloff,[89] V. Demanov,[42] E. Dénes,[9] A. Deppman,[85] G. D'Erasmo,[20] D. Derkach,[30] A. Devaux,[37] D. Di Bari,[20] C. Di Giglio,[20,j] S. Di Liberto,[90] A. Di Mauro,[8] P. Di Nezza,[52] M. Dialinas,[27] L. Díaz,[81] R. Díaz,[32] T. Dietel,[43] R. Divià,[8] Ø. Djuvsland,[19] V. Dobretsov,[16] A. Dobrin,[75] T. Dobrowolski,[89] B. Dönigus,[21] I. Domínguez,[81] D. M. M. Don,[91] O. Dordic,[1] A. K. Dubey,[11] J. Dubuisson,[8] L. Ducroux,[71] P. Dupieux,[37] A. K. Dutta Majumdar,[63] M. R. Dutta Majumdar,[11] D. Elia,[87] D. Emschermann,[66,n] A. Enokizono,[31] B. Espagnon,[56] M. Estienne,[27] S. Esumi,[76] D. Evans,[40] S. Evrard,[8] G. Eyyubova,[1] C. W. Fabjan,[8,o] D. Fabris,[82] J. Faivre,[92] D. Falchieri,[18] A. Fantoni,[52] M. Fasel,[21] O. Fateev,[44] R. Fearick,[67] A. Fedunov,[44] D. Fehlker,[19] V. Fekete,[93] D. Felea,[83] B. Fenton-Olsen,[45,p] G. Feofilov,[30] A. Fernández Téllez,[80] E. G. Ferreiro,[28] A. Ferretti,[35] R. Ferretti,[79,q] M. A. S. Figueredo,[85] S. Filchagin,[42] R. Fini,[87] F. M. Fionda,[20] E. M. Fiore,[20] M. Floris,[88,j] Z. Fodor,[9] S. Foertsch,[67] P. Foka,[21] S. Fokin,[16] F. Formenti,[8] E. Fragiacomo,[94] M. Fragkiadakis,[49] U. Frankenfeld,[21] A. Frolov,[95] U. Fuchs,[8] F. Furano,[8] C. Furget,[92] M. Fusco Girard,[86] J. J. Gaardhøje,[45] S. Gadrat,[92] M. Gagliardi,[35] A. Gago,[69] M. Gallio,[35] P. Ganoti,[49] M. S. Ganti,[11] C. Garabatos,[21] C. García Trapaga,[35] J. Gebelein,[2] R. Gemme,[79] M. Germain,[27] A. Gheata,[8] M. Gheata,[8] B. Ghidini,[20] P. Ghosh,[11] G. Giraudo,[17] P. Giubellino,[17] E. Gladysz-Dziadus,[41] R. Glasow,[43,a] P. Glässel,[66] A. Glenn,[96] R. Gómez Jiménez,[97] H. González Santos,[80] L. H. González-Trueba,[10] P. González-Zamora,[57] S. Gorbunov,[2,c] Y. Gorbunov,[3] S. Gotovac,[98] H. Gottschlag,[43] V. Grabski,[10] R. Grajcarek,[66] A. Grelli,[74] A. Grigoras,[8] C. Grigoras,[8] V. Grigoriev,[58] A. Grigoryan,[5] S. Grigoryan,[44] B. Grinyov,[62] N. Grion,[94] P. Gros,[75] J. F. Grosse-Oetringhaus,[8] J.-Y. Grossiord,[71] R. Grosso,[82] F. Guber,[99] R. Guernane,[92] C. Guerra,[69] B. Guerzoni,[18] K. Gulbrandsen,[45] H. Gulkanyan,[5] T. Gunji,[14] A. Gupta,[51] R. Gupta,[51] H.-A. Gustafsson,[75,a] H. Gutbrod,[21] Ø. Haaland,[19] C. Hadjidakis,[56] M. Haiduc,[83] H. Hamagaki,[14] G. Hamar,[9] J. Hamblen,[100] B. H. Han,[101] J. W. Harris,[29] M. Hartig,[25] A. Harutyunyan,[5] D. Hasch,[52] D. Hasegan,[83] D. Hatzifotiadou,[26] A. Hayrapetyan,[5] M. Heide,[43] M. Heinz,[29] H. Helstrup,[102] A. Herghelegiu,[22] C. Hernández,[21] G. Herrera Corral,[70] N. Herrmann,[66] K. F. Hetland,[102] B. Hicks,[29] A. Hiei,[77] P. T. Hille,[1,r] B. Hippolyte,[47] T. Horaguchi,[77,s] Y. Hori,[14] P. Hristov,[8] I. Hřivnáčová,[56] S. Hu,[103] M. Huang,[19] S. Huber,[21] T. J. Humanic,[23] D. Hutter,[33] D. S. Hwang,[101] R. Ichou,[27] R. Ilkaev,[42] I. Ilkiv,[89] M. Inaba,[76] P. G. Innocenti,[8] M. Ippolitov,[16] M. Irfan,[12] C. Ivan,[74] A. Ivanov,[30] M. Ivanov,[21] V. Ivanov,[50] T. Iwasaki,[77]

A. Jachołkowski,[8] P. Jacobs,[104] L. Jančurová,[44] S. Jangal,[47] R. Janik,[93] C. Jena,[84] S. Jena,[105] L. Jirden,[8] G. T. Jones,[40] P. G. Jones,[40] P. Jovanović,[40] H. Jung,[13] W. Jung,[13] A. Jusko,[40] A. B. Kaidalov,[15] S. Kalcher,[2,c] P. Kaliňák,[38] M. Kalisky,[43] T. Kalliokoski,[32] A. Kalweit,[65] A. Kamal,[12] R. Kamermans,[74] K. Kanaki,[19] E. Kang,[13] J. H. Kang,[60] J. Kapitan,[6] V. Kaplin,[58] S. Kapusta,[8] O. Karavichev,[99] T. Karavicheva,[99] E. Karpechev,[99] A. Kazantsev,[16] U. Kebschull,[2] R. Keidel,[78] M. M. Khan,[12] S. A. Khan,[11] A. Khanzadeev,[50] Y. Kharlov,[59] D. Kikola,[106] B. Kileng,[102] D. J. Kim,[32] D. S. Kim,[13] D. W. Kim,[13] H. N. Kim,[13] J. Kim,[59] J. H. Kim,[101] J. S. Kim,[13] M. Kim,[13] M. Kim,[60] S. H. Kim,[13] S. Kim,[101] Y. Kim,[60] S. Kirsch,[8] I. Kisel,[2,e] S. Kiselev,[15] A. Kisiel,[23,j] J. L. Klay,[107] J. Klein,[66] C. Klein-Bösing,[8,n] M. Kliemant,[25] A. Klovning,[19] A. Kluge,[8] M. L. Knichel,[21] S. Kniege,[25] K. Koch,[66] R. Kolevatov,[1] A. Kolojvari,[30] V. Kondratiev,[30] N. Kondratyeva,[58] A. Konevskih,[99] E. Kornaś,[41] R. Kour,[40] M. Kowalski,[41] S. Kox,[92] K. Kozlov,[16] J. Kral,[54,l] I. Králik,[38] F. Kramer,[25] I. Kraus,[65,e] A. Kravčáková,[61] T. Krawutschke,[108] M. Krivda,[40] D. Krumbhorn,[66] M. Krus,[54] E. Kryshen,[50] M. Krzewicki,[55] Y. Kucheriaev,[16] C. Kuhn,[47] P. G. Kuijer,[55] L. Kumar,[7] N. Kumar,[7] R. Kupczak,[106] P. Kurashvili,[89] A. Kurepin,[99] A. N. Kurepin,[99] A. Kuryakin,[42] S. Kushpil,[6] V. Kushpil,[6] M. Kutouski,[44] H. Kvaerno,[1] M. J. Kweon,[66] Y. Kwon,[60] P. La Rocca,[39,t] F. Lackner,[8] P. Ladrón de Guevara,[57] V. Lafage,[56] C. Lal,[51] C. Lara,[2] D. T. Larsen,[19] G. Laurenti,[26] C. Lazzeroni,[40] Y. Le Bornec,[56] N. Le Bris,[27] H. Lee,[73] K. S. Lee,[13] S. C. Lee,[13] F. Lefèvre,[27] M. Lenhardt,[27] L. Leistam,[8] J. Lehnert,[25] V. Lenti,[87] H. León,[10] I. León Monzón,[97] H. León Vargas,[25] P. Lévai,[9] X. Li,[103] Y. Li,[103] R. Lietava,[40] S. Lindal,[1] V. Lindenstruth,[2,c] C. Lippmann,[8] M. A. Lisa,[23] L. Liu,[19] V. Loginov,[58] S. Lohn,[8] X. Lopez,[37] M. López Noriega,[56] R. López-Ramírez,[80] E. López Torres,[4] G. Løvhøiden,[1] A. Lozea Feijo Soares,[85] S. Lu,[103] M. Lunardon,[53] G. Luparello,[35] L. Luquin,[27] J.-R. Lutz,[47] K. Ma,[68] R. Ma,[29] D. M. Madagodahettige-Don,[91] A. Maevskaya,[99] M. Mager,[65,j] D. P. Mahapatra,[84] A. Maire,[47] I. Makhlyueva,[8] D. Mal'Kevich,[15] M. Malaev,[50] K. J. Malagalage,[3] I. Maldonado Cervantes,[81] M. Malek,[56] L. Malinina,[44,u] T. Malkiewicz,[32] P. Malzacher,[21] A. Mamonov,[42] L. Manceau,[37] L. Mangotra,[51] V. Manko,[16] F. Manso,[37] V. Manzari,[87] Y. Mao,[68,v] J. Mareš,[109] G. V. Margagliotti,[64] A. Margotti,[26] A. Marín,[21] I. Martashvili,[100] P. Martinengo,[8] M. I. Martínez Hernández,[80] A. Martínez Davalos,[10] G. Martínez García,[27] Y. Maruyama,[77] A. Marzari Chiesa,[35] S. Masciocchi,[21] M. Masera,[35] M. Masetti,[18] A. Masoni,[46] L. Massacrier,[71] M. Mastromarco,[87] A. Mastroserio,[20,j] Z. L. Matthews,[40] A. Matyja,[41,w] D. Mayani,[81] G. Mazza,[17] M. A. Mazzoni,[90] F. Meddi,[110] A. Menchaca-Rocha,[10] P. Mendez Lorenzo,[8] M. Meoni,[8] J. Mercado Pérez,[66] P. Mereu,[17] Y. Miake,[76] A. Michalon,[47] N. Miftakhov,[50] L. Milano,[35] J. Milosevic,[1] F. Minafra,[20] A. Mischke,[74] D. Miśkowiec,[21] C. Mitu,[83] K. Mizoguchi,[77] J. Mlynarz,[48] B. Mohanty,[11] L. Molnar,[9,j] M. M. Mondal,[11] L. Montaño Zetina,[70,x] M. Monteno,[17] E. Montes,[57] M. Morando,[53] S. Moretto,[53] A. Morsch,[8] T. Moukhanova,[16] V. Muccifora,[52] E. Mudnic,[98] S. Muhuri,[11] H. Müller,[8] M. G. Munhoz,[85] J. Munoz,[80] L. Musa,[8] A. Musso,[17] B. K. Nandi,[105] R. Nania,[26] E. Nappi,[87] F. Navach,[20] S. Navin,[40] T. K. Nayak,[11] S. Nazarenko,[42] G. Nazarov,[42] A. Nedosekin,[15] F. Nendaz,[71] J. Newby,[96] A. Nianine,[16] M. Nicassio,[87,j] B. S. Nielsen,[45] S. Nikolaev,[16] V. Nikolic,[24] S. Nikulin,[16] V. Nikulin,[50] B. S. Nilsen,[3] M. S. Nilsson,[1] F. Noferini,[26] P. Nomokonov,[44] G. Nooren,[74] N. Novitzky,[32] A. Nyatha,[105] C. Nygaard,[45] A. Nyiri,[1] J. Nystrand,[19] A. Ochirov,[30] G. Odyniec,[104] H. Oeschler,[65] M. Oinonen,[32] K. Okada,[14] Y. Okada,[77] M. Oldenburg,[8] J. Oleniacz,[106] C. Oppedisano,[17] F. Orsini,[36] A. Ortiz Velasquez,[81] G. Ortona,[35] A. Oskarsson,[75] F. Osmic,[8] L. Österman,[75] P. Ostrowski,[106] I. Otterlund,[75] J. Otwinowski,[21] G. Øvrebekk,[19] K. Oyama,[66] K. Ozawa,[14] Y. Pachmayer,[66] M. Pachr,[54] F. Padilla,[35] P. Pagano,[86] G. Paić,[81] F. Painke,[2] C. Pajares,[28] S. Pal,[63,y] S. K. Pal,[11] A. Palaha,[40] A. Palmeri,[34] R. Panse,[2] V. Papikyan,[5] G. S. Pappalardo,[34] W. J. Park,[21] B. Pastirčák,[38] C. Pastore,[87] V. Paticchio,[87] A. Pavlinov,[48] T. Pawlak,[106] T. Peitzmann,[74] A. Pepato,[82] H. Pereira,[36] D. Peressounko,[16] C. Pérez,[69] D. Perini,[8] D. Perrino,[20,j] W. Peryt,[106] J. Peschek,[2,c] A. Pesci,[26] V. Peskov,[81,j] Y. Pestov,[95] A. J. Peters,[8] V. Petráček,[54] A. Petridis,[49,a] M. Petris,[22] P. Petrov,[40] M. Petrovici,[22] C. Petta,[39] J. Peyré,[56] S. Piano,[94] A. Piccotti,[17] M. Pikna,[93] P. Pillot,[27] O. Pinazza,[26,j] L. Pinsky,[91] N. Pitz,[25] F. Piuz,[8] R. Platt,[40] M. Płoskoń,[104] J. Pluta,[106] T. Pocheptsov,[44,z] S. Pochybova,[9] P. L. M. Podesta Lerma,[97] F. Poggio,[35] M. G. Poghosyan,[35] K. Polák,[109] B. Polichtchouk,[59] P. Polozov,[15] V. Polyakov,[50] B. Pommeresch,[19] A. Pop,[22] F. Posa,[20] V. Pospíšil,[54] B. Potukuchi,[51] J. Pouthas,[56] S. K. Prasad,[11] R. Preghenella,[18,t] F. Prino,[17] C. A. Pruneau,[48] I. Pshenichnov,[99] G. Puddu,[88] P. Pujahari,[105] A. Pulvirenti,[39] A. Punin,[42] V. Punin,[42] M. Putiš,[61] J. Putschke,[29] E. Quercigh,[8] A. Rachevski,[94] A. Rademakers,[8] S. Radomski,[66] T. S. Räihä,[32] J. Rak,[32] A. Rakotozafindrabe,[36] L. Ramello,[79] A. Ramírez Reyes,[70] M. Rammler,[43] R. Raniwala,[111] S. Raniwala,[111] S. S. Räsänen,[32] I. Rashevskaya,[94] S. Rath,[84] K. F. Read,[100] J. S. Real,[92] K. Redlich,[89,aa] R. Renfordt,[25] A. R. Reolon,[52] A. Reshetin,[99] F. Rettig,[2,c] J.-P. Revol,[8] K. Reygers,[43,bb] H. Ricaud,[65] L. Riccati,[17] R. A. Ricci,[112] M. Richter,[19] P. Riedler,[8] W. Riegler,[8] F. Riggi,[39] A. Rivetti,[17] M. Rodriguez Cahuantzi,[80] K. Røed,[102] D. Röhrich,[8,cc]

S. Román López,[80] R. Romita,[20,e] F. Ronchetti,[52] P. Rosinský,[8] P. Rosnet,[37] S. Rossegger,[8] A. Rossi,[64,dd] F. Roukoutakis,[8,ee] S. Rousseau,[56] C. Roy,[27,m] P. Roy,[63] A. J. Rubio-Montero,[57] R. Rui,[64] I. Rusanov,[66] G. Russo,[86] E. Ryabinkin,[16] A. Rybicki,[41] S. Sadovsky,[59] K. Šafařík,[8] R. Sahoo,[53] J. Saini,[11] P. Saiz,[8] D. Sakata,[76] C. A. Salgado,[28] R. Salgueiro Domingues da Silva,[8] S. Salur,[104] T. Samanta,[11] S. Sambyal,[51] V. Samsonov,[50] L. Šándor,[38] A. Sandoval,[10] M. Sano,[76] S. Sano,[14] R. Santo,[43] R. Santoro,[20] J. Sarkamo,[32] P. Saturnini,[37] E. Scapparone,[26] F. Scarlassara,[53] R. P. Scharenberg,[113] C. Schiaua,[22] R. Schicker,[66] H. Schindler,[8] C. Schmidt,[21] H. R. Schmidt,[21] K. Schossmaier,[8] S. Schreiner,[8] S. Schuchmann,[25] J. Schukraft,[8] Y. Schutz,[27] K. Schwarz,[21] K. Schweda,[66] G. Scioli,[18] E. Scomparin,[17] P. A. Scott,[40] G. Segato,[53] D. Semenov,[30] S. Senyukov,[79] J. Seo,[13] S. Serci,[88] L. Serkin,[81] E. Serradilla,[57] A. Sevcenco,[83] I. Sgura,[20] G. Shabratova,[44] R. Shahoyan,[8] G. Sharkov,[15] N. Sharma,[7] S. Sharma,[51] K. Shigaki,[77] M. Shimomura,[76] K. Shtejer,[4] Y. Sibiriak,[16] M. Siciliano,[35] E. Sicking,[8,ff] E. Siddi,[46] T. Siemiarczuk,[89] A. Silenzi,[18] D. Silvermyr,[31] E. Simili,[74] G. Simonetti,[20,j] R. Singaraju,[11] R. Singh,[51] V. Singhal,[11] B. C. Sinha,[11] T. Sinha,[63] B. Sitar,[93] M. Sitta,[79] T. B. Skaali,[1] K. Skjerdal,[19] R. Smakal,[54] N. Smirnov,[29] R. Snellings,[55] H. Snow,[40] C. Søgaard,[45] A. Soloviev,[59] H. K. Soltveit,[66] R. Soltz,[96] W. Sommer,[25] C. W. Son,[73] H. Son,[101] M. Song,[60] C. Soos,[8] F. Soramel,[53] D. Soyk,[21] M. Spyropoulou-Stassinaki,[49] B. K. Srivastava,[113] J. Stachel,[66] F. Staley,[36] E. Stan,[83] G. Stefanek,[89] G. Stefanini,[8] T. Steinbeck,[2,c] E. Stenlund,[75] G. Steyn,[67] D. Stocco,[35,w] R. Stock,[25] P. Stolpovsky,[59] P. Strmen,[93] A. A. P. Suaide,[85] M. A. Subieta Vásquez,[35] T. Sugitate,[77] C. Suire,[56] M. Šumbera,[6] T. Susa,[24] D. Swoboda,[8] J. Symons,[104] A. Szanto de Toledo,[85] I. Szarka,[93] A. Szostak,[46] M. Szuba,[106] M. Tadel,[8] C. Tagridis,[49] A. Takahara,[14] J. Takahashi,[72] R. Tanabe,[76] J. D. Tapia Takaki,[56] H. Taureg,[8] A. Tauro,[8] M. Tavlet,[8] G. Tejeda Muñoz,[80] A. Telesca,[8] C. Terrevoli,[20] J. Thäder,[2,c] R. Tieulent,[71] D. Tlusty,[54] A. Toia,[8] T. Tolyhy,[9] C. Torcato de Matos,[8] H. Torii,[77] G. Torralba,[2] L. Toscano,[17] F. Tosello,[17] A. Tournaire,[27,gg] T. Traczyk,[106] P. Tribedy,[11] G. Tröger,[2] D. Truesdale,[23] W. H. Trzaska,[32] G. Tsiledakis,[66] E. Tsilis,[49] T. Tsuji,[14] A. Tumkin,[42] R. Turrisi,[82] A. Turvey,[3] T. S. Tveter,[1] H. Tydesjö,[8] K. Tywoniuk,[1] J. Ulery,[25] K. Ullaland,[19] A. Uras,[88] J. Urbán,[61] G. M. Urciuoli,[90] G. L. Usai,[88] A. Vacchi,[94] M. Vala,[44,hh] L. Valencia Palomo,[10] S. Vallero,[66] N. van der Kolk,[55] P. Vande Vyvre,[8] M. van Leeuwen,[74] L. Vannucci,[112] A. Vargas,[80] R. Varma,[105] A. Vasiliev,[16] I. Vassiliev,[2,ee] M. Vasileiou,[49] V. Vechernin,[30] M. Venaruzzo,[64] E. Vercellin,[35] S. Vergara,[80] R. Vernet,[39,ii] M. Verweij,[74] I. Vetlitskiy,[15] L. Vickovic,[98] G. Viesti,[53] O. Vikhlyantsev,[42] Z. Vilakazi,[67] O. Villalobos Baillie,[40] A. Vinogradov,[16] L. Vinogradov,[30] Y. Vinogradov,[42] T. Virgili,[86] Y. P. Viyogi,[11] A. Vodopianov,[44] K. Voloshin,[15] S. Voloshin,[48] G. Volpe,[20] B. von Haller,[8] D. Vranic,[21] J. Vrláková,[61] B. Vulpescu,[37] B. Wagner,[19] V. Wagner,[54] L. Wallet,[8] R. Wan,[68,m] D. Wang,[68] Y. Wang,[66] Y. Wang,[68] K. Watanabe,[76] Q. Wen,[103] J. Wessels,[43] U. Westerhoff,[43] J. Wiechula,[66] J. Wikne,[1] A. Wilk,[43] G. Wilk,[89] M. C. S. Williams,[26] N. Willis,[56] B. Windelband,[66] C. Xu,[68] C. Yang,[68] H. Yang,[66] S. Yasnopolskiy,[16] F. Yermia,[27] J. Yi,[73] Z. Yin,[68] H. Yokoyama,[76] I-K. Yoo,[73] X. Yuan,[68,jj] V. Yurevich,[44] I. Yushmanov,[16] E. Zabrodin,[1] B. Zagreev,[15] A. Zalite,[50] C. Zampolli,[8,kk] Yu. Zanevsky,[44] S. Zaporozhets,[44] A. Zarochentsev,[30] P. Závada,[109] H. Zbroszczyk,[106] P. Zelnicek,[2] A. Zenin,[59] A. Zepeda,[70] I. Zgura,[83] M. Zhalov,[50] X. Zhang,[68,b] D. Zhou,[68] S. Zhou,[103] J. Zhu,[68] A. Zichichi,[18,t] A. Zinchenko,[44] G. Zinovjev,[62] Y. Zoccarato,[71] V. Zycháček,[54] and M. Zynovyev[62]

(ALICE Collaboration)

[1]*Department of Physics, University of Oslo, Oslo, Norway*
[2]*Kirchhoff-Institut für Physik, Ruprecht-Karls-Universität Heidelberg, Heidelberg, Germany*
[3]*Physics Department, Creighton University, Omaha, Nebraska, USA*
[4]*Centro de Aplicaciones Tecnológicas y Desarrollo Nuclear (CEADEN), Havana, Cuba*
[5]*Yerevan Physics Institute, Yerevan, Armenia*
[6]*Nuclear Physics Institute, Academy of Sciences of the Czech Republic, Řež u Prahy, Czech Republic*
[7]*Physics Department, Panjab University, Chandigarh, India*
[8]*European Organization for Nuclear Research (CERN), Geneva, Switzerland*
[9]*KFKI Research Institute for Particle and Nuclear Physics, Hungarian Academy of Sciences, Budapest, Hungary*
[10]*Instituto de Física, Universidad Nacional Autónoma de México, Mexico City, Mexico*
[11]*Variable Energy Cyclotron Centre, Kolkata, India*
[12]*Department of Physics, Aligarh Muslim University, Aligarh, India*
[13]*Gangneung-Wonju National University, Gangneung, South Korea*
[14]*University of Tokyo, Tokyo, Japan*
[15]*Institute for Theoretical and Experimental Physics, Moscow, Russia*
[16]*Russian Research Centre Kurchatov Institute, Moscow, Russia*

[17]*Sezione INFN, Turin, Italy*
[18]*Dipartimento di Fisica dell'Università and Sezione INFN, Bologna, Italy*
[19]*Department of Physics and Technology, University of Bergen, Bergen, Norway*
[20]*Dipartimento Interateneo di Fisica 'M. Merlin' andSezione INFN, Bari, Italy*
[21]*Research Division and ExtreMe Matter Institute EMMI, GSI Helmholtzzentrum für Schwerionenforschung, Darmstadt, Germany*
[22]*National Institute for Physics and Nuclear Engineering, Bucharest, Romania*
[23]*Department of Physics, The Ohio State University, Columbus, Ohio, USA*
[24]*Rudjer Bošković Institute, Zagreb, Croatia*
[25]*Institut für Kernphysik, Johann Wolfgang Goethe-Universität Frankfurt, Frankfurt, Germany*
[26]*Sezione INFN, Bologna, Italy*
[27]*SUBATECH, Ecole des Mines de Nantes, Université de Nantes, CNRS-IN2P3, Nantes, France*
[28]*Departamento de Física de Partículas and IGFAE, Universidad de Santiago de Compostela, Santiago de Compostela, Spain*
[29]*Yale University, New Haven, Connecticut, USA*
[30]*V. Fock Institute for Physics, St. Petersburg State University, St. Petersburg, Russia*
[31]*Oak Ridge National Laboratory, Oak Ridge, Tennessee, USA*
[32]*Helsinki Institute of Physics (HIP) and University of Jyväskylä, Jyväskylä, Finland*
[33]*Frankfurt Institute for Advanced Studies, Johann Wolfgang Goethe-Universität Frankfurt, Frankfurt, Germany*
[34]*Sezione INFN, Catania, Italy*
[35]*Dipartimento di Fisica Sperimentale dell'Università and Sezione INFN, Turin, Italy*
[36]*Commissariat à l'Energie Atomique, IRFU, Saclay, France*
[37]*Laboratoire de Physique Corpusculaire (LPC), Clermont Université, Université Blaise Pascal, CNRS-IN2P3, Clermont-Ferrand, France*
[38]*Institute of Experimental Physics, Slovak Academy of Sciences, Košice, Slovakia*
[39]*Dipartimento di Fisica e Astronomia dell'Università and Sezione INFN, Catania, Italy*
[40]*School of Physics and Astronomy, University of Birmingham, Birmingham, United Kingdom*
[41]*The Henryk Niewodniczanski Institute of Nuclear Physics, Polish Academy of Sciences, Cracow, Poland*
[42]*Russian Federal Nuclear Center (VNIIEF), Sarov, Russia*
[43]*Institut für Kernphysik, Westfälische Wilhelms-Universität Münster, Münster, Germany*
[44]*Joint Institute for Nuclear Research (JINR), Dubna, Russia*
[45]*Niels Bohr Institute, University of Copenhagen, Copenhagen, Denmark*
[46]*Sezione INFN, Cagliari, Italy*
[47]*Institut Pluridisciplinaire Hubert Curien (IPHC), Université de Strasbourg, CNRS-IN2P3, Strasbourg, France*
[48]*Wayne State University, Detroit, Michigan, USA*
[49]*Physics Department, University of Athens, Athens, Greece*
[50]*Petersburg Nuclear Physics Institute, Gatchina, Russia*
[51]*Physics Department, University of Jammu, Jammu, India*
[52]*Laboratori Nazionali di Frascati, INFN, Frascati, Italy*
[53]*Dipartimento di Fisica dell'Università and Sezione INFN, Padova, Italy*
[54]*Faculty of Nuclear Sciences and Physical Engineering, Czech Technical University in Prague, Prague, Czech Republic*
[55]*Nikhef, National Institute for Subatomic Physics, Amsterdam, Netherlands*
[56]*Institut de Physique Nucléaire d'Orsay (IPNO), Université Paris-Sud, CNRS-IN2P3, Orsay, France*
[57]*Centro de Investigaciones Energéticas Medioambientales y Tecnológicas (CIEMAT), Madrid, Spain*
[58]*Moscow Engineering Physics Institute, Moscow, Russia*
[59]*Institute for High Energy Physics, Protvino, Russia*
[60]*Yonsei University, Seoul, South Korea*
[61]*Faculty of Science, P.J. Šafárik University, Košice, Slovakia*
[62]*Bogolyubov Institute for Theoretical Physics, Kiev, Ukraine*
[63]*Saha Institute of Nuclear Physics, Kolkata, India*
[64]*Dipartimento di Fisica dell'Università and Sezione INFN, Trieste, Italy*
[65]*Institut für Kernphysik, Technische Universität Darmstadt, Darmstadt, Germany*
[66]*Physikalisches Institut, Ruprecht-Karls-Universität Heidelberg, Heidelberg, Germany*
[67]*Physics Department, University of Cape Town, iThemba Laboratories, Cape Town, South Africa*
[68]*Hua-Zhong Normal University, Wuhan, China*
[69]*Sección Física, Departamento de Ciencias, Pontificia Universidad Católica del Perú, Lima, Peru*
[70]*Centro de Investigación y de Estudios Avanzados (CINVESTAV), Mexico City and Mérida, Mexico*
[71]*Université de Lyon, Université Lyon 1, CNRS/IN2P3, IPN-Lyon, Villeurbanne, France*
[72]*Universidade Estadual de Campinas (UNICAMP), Campinas, Brazil*
[73]*Pusan National University, Pusan, South Korea*
[74]*Nikhef and Institute for Subatomic Physics of Utrecht University, Utrecht, Netherlands*
[75]*Division of Experimental High Energy Physics, University of Lund, Lund, Sweden*
[76]*University of Tsukuba, Tsukuba, Japan*

[77]*Hiroshima University, Hiroshima, Japan*
[78]*Zentrum für Technologietransfer und Telekommunikation (ZTT), Fachhochschule Worms, Worms, Germany*
[79]*Dipartimento di Scienze e Tecnologie Avanzate dell'Università del Piemonte Orientale and Gruppo Collegato INFN, Alessandria, Italy*
[80]*Benemérita Universidad Autónoma de Puebla, Puebla, Mexico*
[81]*Instituto de Ciencias Nucleares, Universidad Nacional Autónoma de México, Mexico City, Mexico*
[82]*Sezione INFN, Padova, Italy*
[83]*Institute of Space Sciences (ISS), Bucharest, Romania*
[84]*Institute of Physics, Bhubaneswar, India*
[85]*Universidade de São Paulo (USP), São Paulo, Brazil*
[86]*Dipartimento di Fisica 'E.R. Caianiello' dell'Università and Sezione INFN, Salerno, Italy*
[87]*Sezione INFN, Bari, Italy*
[88]*Dipartimento di Fisica dell'Università and Sezione INFN, Cagliari, Italy*
[89]*Soltan Institute for Nuclear Studies, Warsaw, Poland*
[90]*Sezione INFN, Rome, Italy*
[91]*University of Houston, Houston, Texas, USA*
[92]*Laboratoire de Physique Subatomique et de Cosmologie (LPSC), Université Joseph Fourier, CNRS-IN2P3, Institut Polytechnique de Grenoble, Grenoble, France*
[93]*Faculty of Mathematics, Physics and Informatics, Comenius University, Bratislava, Slovakia*
[94]*Sezione INFN, Trieste, Italy*
[95]*Budker Institute for Nuclear Physics, Novosibirsk, Russia*
[96]*Lawrence Livermore National Laboratory, Livermore, California, USA*
[97]*Universidad Autónoma de Sinaloa, Culiacán, Mexico*
[98]*Technical University of Split FESB, Split, Croatia*
[99]*Institute for Nuclear Research, Academy of Sciences, Moscow, Russia*
[100]*University of Tennessee, Knoxville, Tennessee, USA*
[101]*Department of Physics, Sejong University, Seoul, South Korea*
[102]*Faculty of Engineering, Bergen University College, Bergen, Norway*
[103]*China Institute of Atomic Energy, Beijing, China*
[104]*Lawrence Berkeley National Laboratory, Berkeley, California, USA*
[105]*Indian Institute of Technology, Mumbai, India*
[106]*Warsaw University of Technology, Warsaw, Poland*
[107]*California Polytechnic State University, San Luis Obispo, California, USA*
[108]*Fachhochschule Köln, Köln, Germany*
[109]*Institute of Physics, Academy of Sciences of the Czech Republic, Prague, Czech Republic*
[110]*Dipartimento di Fisica dell'Università 'La Sapienza' and Sezione INFN, Rome, Italy*
[111]*Physics Department, University of Rajasthan, Jaipur, India*
[112]*Laboratori Nazionali di Legnaro, INFN, Legnaro, Italy*
[113]*Purdue University, West Lafayette, Indiana, USA*

[a]Deceased.
[b]Also at Laboratoire de Physique Corpusculaire (LPC), Clermont Université, Université Blaise Pascal, CNRS-IN2P3, Clermont-Ferrand, France.
[c]Also at Frankfurt Institute for Advanced Studies, Johann Wolfgang Goethe-Universität Frankfurt, Frankfurt, Germany.
[d]Now at Sezione INFN, Padova, Italy.
[e]Now at Research Division and ExtreMe Matter Institute EMMI, GSI Helmholtzzentrum für Schwerionenforschung, Darmstadt, Germany.
[f]Now at Institut für Kernphysik, Johann Wolfgang Goethe-Universität Frankfurt, Frankfurt, Germany.
[g]Now at Physics Department, University of Cape Town, iThemba Laboratories, Cape Town, South Africa.
[h]Now at National Institute for Physics and Nuclear Engineering, Bucharest, Romania.
[i]Also at University of Houston, Houston, TX, USA.
[j]Now at European Organization for Nuclear Research (CERN), Geneva, Switzerland.
[k]Also at Dipartimento di Fisica dell'Università, Udine, Italy.
[l]Now at Helsinki Institute of Physics (HIP) and University of Jyväskylä, Jyväskylä, Finland.
[m]Now at Institut Pluridisciplinaire Hubert Curien (IPHC), Université de Strasbourg, CNRS-IN2P3, Strasbourg, France.
[n]Now at Institut für Kernphysik, Westfälische Wilhelms-Universität Münster, Münster, Germany.
[o]Now at University of Technology and Austrian Academy of Sciences, Vienna, Austria.
[p]Also at Lawrence Livermore National Laboratory, Livermore, CA, USA.
[q]Also at European Organization for Nuclear Research (CERN), Geneva, Switzerland.

[r]Now at Yale University, New Haven, CT, USA.
[s]Now at University of Tsukuba, Tsukuba, Japan.
[t]Also at Centro Fermi–Centro Studi e Ricerche e Museo Storico della Fisica ''Enrico Fermi,'' Rome, Italy.
[u]Also at Moscow State University, Moscow, Russia.
[v]Also at Laboratoire de Physique Subatomique et de Cosmologie (LPSC), Université Joseph Fourier, CNRS-IN2P3, Institut Polytechnique de Grenoble, Grenoble, France.
[w]Now at SUBATECH, Ecole des Mines de Nantes, Université de Nantes, CNRS-IN2P3, Nantes, France.
[x]Now at Dipartimento di Fisica Sperimentale dell'Università and Sezione INFN, Turin, Italy.
[y]Now at Commissariat à l'Energie Atomique, IRFU, Saclay, France.
[z]Also at Department of Physics, University of Oslo, Oslo, Norway.
[aa]Also at Wrocław University, Wrocław, Poland.
[bb]Now at Physikalisches Institut, Ruprecht-Karls-Universität Heidelberg, Heidelberg, Germany.
[cc]Now at Department of Physics and Technology, University of Bergen, Bergen, Norway.
[dd]Now at Dipartimento di Fisica dell'Università and Sezione INFN, Padova, Italy.
[ee]Now at Physics Department, University of Athens, Athens, Greece.
[ff]Also at Institut für Kernphysik, Westfälische Wilhelms-Universität Münster, Münster, Germany.
[gg]Now at Université de Lyon, Université Lyon 1, CNRS/IN2P3, IPN-Lyon, Villeurbanne, France.
[hh]Now at Faculty of Science, P.J. Šafárik University, Košice, Slovakia.
[ii]Now at Centre de Calcul IN2P3, Lyon, France.
[jj]Also at Dipartimento di Fisica dell'Università and Sezione INFN, Padova, Italy.
[kk]Also at Sezione INFN, Bologna, Italy.